European Journal of Medicinal Chemistry 46 (2011) 4573–4583

Contents lists available at ScienceDirect

European Journal of Medicinal Chemistry

journal homepage: http://www.elsevier.com/locate/ejmech

Original article

6-Substituted imidazo[1,2-*a*]pyridines: Synthesis and biological activity against colon cancer cell lines HT-29 and Caco-2

Nurit Dahan-Farkas [a], Candice Langley [b], Amanda L. Rousseau [b], Dharmendra B. Yadav [b], Hajierah Davids [a,c,**], Charles B. de Koning [b,*]

[a] Division of Pharmacology, Department of Pharmacy and Pharmacology, Faculty of Health Sciences, University of the Witwatersrand, 7 York Road, Parktown 2193, South Africa
[b] Molecular Sciences Institute, School of Chemistry, University of the Witwatersrand, P.O. Wits 2050, South Africa
[c] Department of Biochemistry & Microbiology, Nelson Mandela Metropolitan University, P.O. Box 77000, Port Elizabeth 6031, South Africa

ARTICLE INFO

Article history:
Received 23 May 2011
Received in revised form
20 July 2011
Accepted 20 July 2011
Available online 27 July 2011

Keywords:
6-substituted imidazo[1,2-*a*]pyridines
Multicomponent coupling reactions
Colon cancer
HT-29 and Caco-2
Apoptosis
Caspases

ABSTRACT

A range of 6-substituted imidazo[1,2-*a*]pyridines were synthesized using a multicomponent coupling reaction. Most of these compounds were found to exhibit excellent activity against the colon cancer cell lines HT-29 and Caco-2, whilst not showing significant toxicity against white blood cells. Our studies have shown that the proteolytic phase of apoptosis was initiated 2 h after treatment with these imidazo−[1,2-*a*]pyridines. The data suggests that the imidazo[1,2-*a*]pyridine-induced cell death in HT-29 and Caco-2 cells is mediated via pathway(s) that include the release of cytochrome *c* from the mitochondria to the cytosol and the activation of caspase 3 and caspase 8.

1. Introduction

Cancer continues to pose significant health problems worldwide, despite medical advances that have, over the last decade, increased our understanding of the genetics of cancer and the application of novel drug therapy. Approximately 782 000 people are diagnosed with colon cancer annually. In the United States, colon cancer is the third most common cause of cancer-related deaths with an estimated annual incidence of 146 970 and a mortality of 49 920 reported in 2009 [1]. Conventional treatment of colon cancer is by surgical ablation, with chemotherapy and/or radiotherapy used as adjunctive treatment, as over 40% of colon cancer patients develop metastases. These approaches are not always effective against the highly metastasised disease and hence, new therapeutic methods are essential for treatment [2].

Cellular homeostasis is maintained by a balance between cell proliferation and cell death, with the latter constituting one of the major targets in medical research. Cell injury can lead to cell death by necrosis or apoptosis. Apoptosis is characterised by various morphological changes, including plasma membrane blebbing, chromatin condensation, nuclear fragmentation and formation of apoptotic bodies [3]. In addition, biochemical features of apoptosis such as the exposure of phosphatidylserine (PS) on the outer leaflet of the plasma membrane [4], changes to the permeability of the mitochondrial membrane [5], and the release of proteins such as cytochrome *c* from the mitochondrial intermembrane space are noted [6].

There are several factors involved in the apoptotic process, including the co-ordinated action of a cascade of initiator or effector caspases (cysteine aspartate-specific proteases) [7]. Caspase activation leads to the various morphological and biochemical features of apoptosis. Caspase 3 is the key effector caspase responsible for the cleavage of multiple protein substrates in the cells, ultimately leading to apoptosis. Opening of the mitochondrial permeability transition (MPT) pore causes a loss of the inner mitochondrial membrane potential ($\Delta\psi_m$), leading to the release of cytochrome *c* from the mitochondrial intermembrane space. Cytochrome *c* then binds to apoptotic protease activating factor 1

* Corresponding author. Tel.: +27 11 7176724; fax: +27 11 7176749.
** Corresponding author. Division of Pharmacology, Department of Pharmacy and Pharmacology, Faculty of Health Sciences, University of the Witwatersrand, 7 York Road, Parktown 2193, South Africa. Tel.: +27 41 504 2019; fax: +27 41 504 2814.
E-mail addresses: Candice.Langley@gmail.com (C. Langley), Amanda.Rousseau@wits.ac.za (A.L. Rousseau), Dharmendra.Yadav@wits.ac.za (D.B. Yadav), Hajierah.Davids@nmmu.ac.za (H. Davids), Charles.deKoning@wits.ac.za (C.B. de Koning).

0223-5234/$ – see front matter © 2011 Elsevier Masson SAS. All rights reserved.
doi:10.1016/j.ejmech.2011.07.036

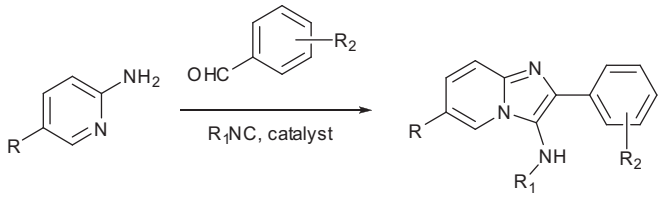

Scheme 1. Three component coupling reaction for the synthesis of imidazo[1,2-*a*] pyridines.

(Apaf-1) and activated caspase 3, which results in mitochondrial-dependent apoptosis [8,9].

In cancerous cells, there are very low levels of apoptosis and DNA repair seldom occurs. Several chemotherapeutic agents have been shown to be effective inducers of apoptosis through underlying cellular mechanisms. The identification of inducers of apoptosis presents a strong basis for the development of potential anticancer agents and through the induction of apoptosis, novel compounds may reduce the resistance of colon cancer cells to current therapeutic regimes [10].

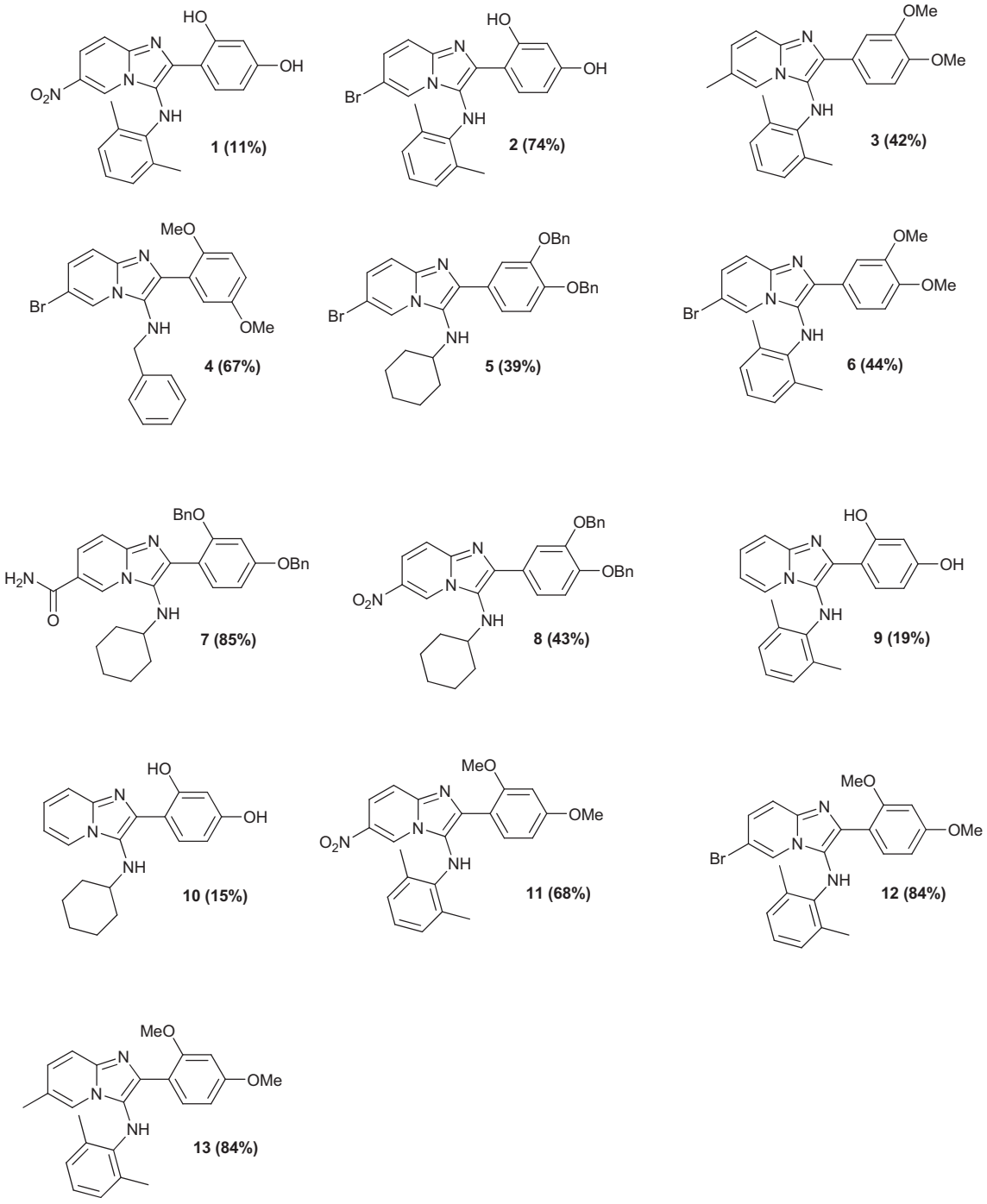

Fig. 1. Imidazo[1,2-*a*]pyridines **1**–**13** and percentage yields.

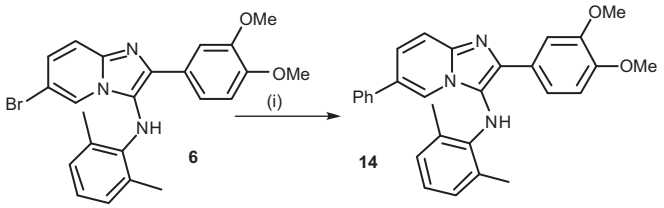

Scheme 2. *Reagents and conditions* (i) 10% $Pd(PPh_3)_4$, $PhB(OH)_2$, CsF, DME, Discovery microwave, 150 °C and 150 W, 20 min, 95%.

In recent times, the use of multicomponent coupling reactions [11] in the synthesis of compounds displaying interesting pharmacological properties has been an area of prolific research. One of the classes of compounds that are accessible by multicomponent coupling reactions are the imidazo[1,2-*a*]pyridines [12–20].

In the present study, we synthesized a number of novel imidazo[1,2-*a*]pyridines and then assessed the anticancer properties of these imidazopyridines against two colon cancer cell lines, aiming to investigate any cytotoxic effects on the cells, the mode of cell death, and to explore the pathways by which cell death was induced.

2. Results and discussion

2.1. Chemistry

Using methodology previously described [14], a series of novel 6-substituted imidazo[1,2-*a*]pyridines were prepared from a variety of commercially available 5-substituted 2-aminopyridines with either benzyl isocyanide, cyclohexyl isocyanide or 2,6-dimethylphenyl isocyanide, and a variety of substituted aromatic aldehydes in the presence of montmorillonite clay K10 (Scheme 1). In addition, two imidazo[1,2-*a*]pyridines lacking a substituent in the 6-position were also prepared by this method (R = H, Scheme 1). This facile, one-pot reaction afforded imidazo[1,2-*a*]pyridines **1**–**13** in the unoptimized yields shown in Fig. 1. All products were characterised by ^1H, ^{13}C NMR spectroscopy as well as by HRMS.

A number of the imidazo[1,2-*a*]pyridines prepared contain an aromatic bromine substituent, and we envisaged using this as a handle for carbon–carbon coupling reactions such as the Suzuki–Miyaura reaction. Using this methodology, further variety could be introduced onto the imidazo[1,2-*a*]pyridine nucleus. For example, exposure of **6** to phenylboronic acid in the presence of catalytic $Pd(PPh_3)_4$ in a microwave afforded **14** in a yield of 95% (Scheme 2).

Table 1
Percentage cell viability of HT-29 and Caco-2 treated with 100 μM of the imidazopyridines and camptothecin, for 24 h.

Compound	Cell Viability % (100 μM)	
	HT-29	Caco-2
1	118.79 ± 1.13	113.43 ± 1.01
2	108.30 ± 0.69	109.77 ± 1.42
3	17.08 ± 1.03	15.68 ± 2.27
4	8.64 ± 0.84	9.47 ± 1.41
5	86.46 ± 1.09	90.32 ± 0.74
6	11.44 ± 0. 20	10.77 ± 0.17
7	6.81 ± 0.36	6.45 ± 1.76
8	93.71 ± 1.12	89.27 ± 0.45
9	79.48 ± 0.93	82.53 ± 2.16
10	86.92 ± 1.33	82.95 ± 0.84
11	82.46 ± 0.74	88.62 ± 1.03
12	17.19 ± 0.95	19.78 ± 1.32
13	11.37 ± 1.20	13.58 ± 0.56
14	10.67 ± 0.80	12.94 ± 0.2
Camptothecin	12.79 ± 1.56	13.94 ± 1.54

Table 2
IC_{50} values for the imidazopyridines and camptothecin on the Caco-2 and HT-29 cell lines.

Compound	IC_{50} (μM)	
	HT-29	Caco-2
3	12.89 ± 2.41	11.91 ± 1.10
4	6.57 ± 1.91	6.43 ± 1.01
6	9.14 ± 1.02	9.03 ± 0.99
7	9.20 ± 0.83	17.38 ± 1.13
12	21.98 ± 1.17	20.28 ± 3.45
13	10.03 ± 2.69	15.02 ± 1.98
14	8.56 ± 1.22	8.73 ± 1.28
Camptothecin	10.00 ± 1.41	9.55 ± 2.21

2.2. Pharmacology

A number of cell viability and flow cytometry assays were used to determine whether imidazo[1,2-*a*]pyridines **1**–**14** induced cell death in colon cancer cell lines.

2.2.1. Effect of imidazo[1,2-a]pyridines on HT-29 and Caco-2 cell proliferation

The effect of imidazo[1,2-*a*]pyridines **1**–**14** on HT-29 and Caco-2 cell proliferation was accomplished by exposing a cell population to compounds **1**–**14** and then monitoring the mitochondrial enzymatic reduction of MTT to formazan. The colon cancer cells were initially exposed to all imidazo[1,2-*a*]pyridines at 100 μM (final concentration in the well) at 37 °C for 24 h. The MTT assay was used to quantify cell viability after exposure (Table 1). A compound was considered active if it reduced the growth of the cell lines to 50% or less. Interestingly, structure–activity relationships became apparent from our small set of imidazo[1,2-*a*]pyridines. All of the compounds bearing a nitro substituent in the 6-position of the imidazopyridine nucleus and all those bearing a 2,5-dihydroxyphenyl substituent attached to the imidazopyridine showed little reduction of cell growth of both colon cancer cell lines. Conversely, imidazopyridines containing protected hydroxyl substituents on the benzene ring generally displayed good activities. Therefore, only imidazo[1,2-*a*]pyridines **3**, **4**, **6**, **7** and **12**–**14** showing >50% reduction in cell viability were tested further.

The IC_{50} values (micromolar concentration that inhibited growth by 50%) obtained from the active imidazo[1,2-*a*]pyridines **3**, **4**, **6**, **7** and **12**–**14** are reported in Table 2. IC_{50} values showed no significant difference ($p = 0.665$) between compounds **6** (9.14 ± 1.02 μM), **7** (9.20 ± 0.83 μM), **13** (10.03 ± 2.69 μM), **14** (8.56 ± 1.22 μM) and camptothecin (9.99 ± 1.41 μM) on the HT-29 cells, while compounds **12** and **3** showed significantly ($p = 0.005$) higher IC_{50} values of 21.98 ± 1.17 μM and 12.89 ± 2.41 μM respectively.

Table 3
Percentage cell viability of the white blood cells treated with 100 μM imidazopyridines or camptothecin, for 24 h.

Compound	White Blood Cell Viability %
3	76.176 ± 0.567%
4	88.943 ± 1.996%
6	83.762 ± 1.389%
7	93.834 ± 0.271%
12	96.311 ± 5.023%
13	97.479 ± 1.178%
14	77.345 ± 1.005%
Camptothecin	33.782 ± 2.031%

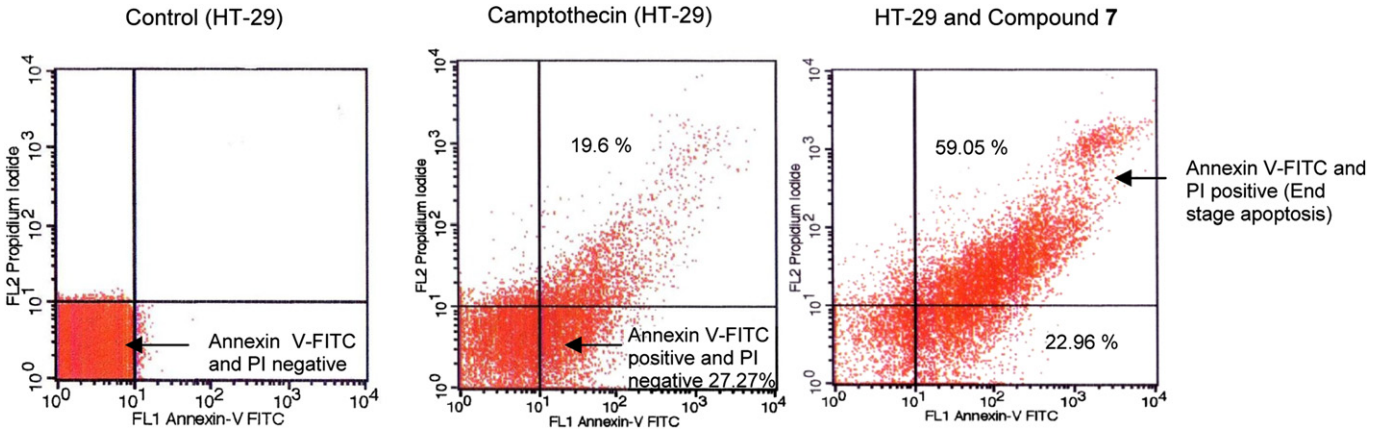

Fig. 2. Analysis of apoptosis induced by compound **7** in the HT-29 colon cancer cell line.

IC_{50} values determined for imidazopyridines **3**, **7**, **12** and **13** on the Caco-2 cell line were significantly higher ($p = 0.001$) than for camptothecin (9.55 ± 2.21 μM), while those obtained for compounds **6** and **14** were comparable with camptothecin. Compound **4** was more effective than camptothecin in inhibiting both Caco-2 and HT-29 growth.

2.2.2. Effects on cell viability of white blood cells

Freshly isolated white blood cells were exposed to a range of active imidazopyridines at a final well concentration of 100 μM for 24 h. Cell viability was determined by the MTT assay. The results obtained are summarized in Table 3. The prepared imidazopyridines showed significantly lower cytotoxicity towards the white blood cells than 100 μM camptothecin ($p = 0.0001$). This suggests that the imidazo[1,2-*a*]pyridines considered in this study may be more selective than camptothecin.

2.2.3. Effects on cell death of HT-29 and Caco-2 cells

Vermes et al. [21] reported that translocation of phosphatidylserine (PS) from the inner side of the plasma membrane to the outer layer occurs in the early stage of apoptosis. The apoptosis assay monitors cell membrane translocation events and the accessibility of nuclear material in response to extracellular disruptions, with the various stages of apoptosis being quantified by flow cytometry.

Our results show that apoptosis was induced after addition of the imidazopyridines in both colon cancer cell lines, as shown in the representative example of compound **7** compared to camptothecin in the HT-29 colon cancer cell line, shown in Fig. 2.

Apoptosis differs from necrosis in that during the initial stages of apoptosis, the cell membrane remains intact, whilst the cell membrane loses its integrity during necrosis. The apoptotic nature of the imidazo[1,2-*a*]pyridine-induced cell death was confirmed by annexin V-FITC labelling of PS exposed on the plasma membrane. The extent to which annexin V-FITC binds to the cell surface was measured in conjunction with a propidium iodide (PI) exclusion test to investigate the integrity of the cell membrane. The untreated cells (control) were annexin V-FITC and PI negative, indicating that they were viable and not undergoing apoptosis.

After a 24 h exposure to the imidazo[1,2-*a*]pyridines or camptothecin, there were primarily two populations of cells: viable, non-apoptosing cells (annexin V-FITC and PI negative) and cells undergoing apoptosis (annexin V-FITC positive and PI negative). A small population of cells was observed to be annexin V-FITC and PI positive, indicating that they were in end-stage apoptosis. The percentage of each subpopulation of cells in both cell lines exposed to the imidazo[1,2-*a*]pyridines is summarized in Table 4.

2.2.4. Enzyme activity assays

During the process of apoptosis, the initiation of all intracellular events is linked to the activation of caspases. All of the caspases promote apoptosis through the proteolytic degradation of cellular components. Caspase 8, a member of the caspase family, is crucial for cell death induction. Impaired expression or function of caspase 8 can promote tumour formation, progression and treatment resistance in several types of cancers [22]. Caspase 8 is an initiator caspase which cleaves and activates the effector caspases (e.g. caspase 3). Once activated, caspase 3, the key executioner of apoptosis, is responsible for the cleavage and breakdown of several cellular components related to DNA repair and regulation, and cleaves polypeptides that ultimately undergo proteolysis in apoptotic cells. To determine the involvement of caspase 3 and caspase 8 in the imidazo[1,2-*a*]pyridine-induced apoptosis, caspase-specific colorimetric assays were used to measure caspase activity. The level of caspase activity in the cell lysate is directly proportional to the absorbance of *p*-nitroaniline (pNA) for caspase 3 and caspase 8 at 405 nm.

In this study, it was noted that treatment with the selected imidazo[1,2-*a*]pyridines induced caspase 8 and caspase 3 activity in both colon cancer cell lines at a concentration of 100 μM. A time-dependent activation of caspase 3 was found through 24 h of exposure to the imidazo[1,2-*a*]pyridines after which the activity diminished. The reduction of the caspase 3 activity at 24 h is possibly due to the cytotoxic effects of the imidazopyridines resulting in the death of cells.

Table 4
Analysis of apoptosis induced by the imidazo[1,2-*a*]pyridines in the HT-29 and Caco-2 cell lines.

Compound	Viable cells (%)		Early apoptosis (%)		Late apoptosis (%)	
	HT-29	Caco-2	HT-29	Caco-2	HT-29	Caco-2
3	12.53	13.21	18.11	21.85	60.98	56.31
4	16.53	23.88	28.18	25.87	47.22	44.77
6	12.11	17.47	18.29	15.97	66.54	57.23
7	14.48	20.27	22.96	18.67	59.05	53.8
12	38.57	44.40	42.71	25.02	15.75	18.67
13	18.51	13.97	43.28	19.93	30.8	59.81
14	50.18	15.55	27.06	18.99	17.78	60.05
Camptothecin	47.95	50.18	27.27	27.06	19.64	17.78

For example, the exposure of the HT-29 cell line to imidazopyridine **7** resulted in maximal caspase 8 activity within 2 h, as shown in Fig. 3. After 2 h, the activity of caspase 8 declined whereas that of caspase 3 increased, indicating that the proteolytic phase of apoptosis was initiated. By comparison, maximal caspase 8 activity was observed in the HT-29 cells within 2 h of exposure to compounds **4** (Fig. 3), **6** and **14**, and within 4 h of exposure to compounds **3, 12** and **13**.

Similar trends were observed with the executioner caspase, caspase 3, with maximum levels in HT-29 cells observed after 2 h of exposure to compounds **4** (Fig. 3), **6** and **14**. Caspase 3 activity in HT-29 cells treated with compound **3** reached a maximum after 4 h of exposure, while maximum levels were observed between 2 and 4 h after exposure to compound **13**, and between 2 h and 8 h after exposure to compound **12** (figures not shown). These high levels of caspase 3 activity indicate that apoptosis was initiated fairly early after exposure to these compounds. Camptothecin was also tested in the time-dependent induction of caspase 3 and 8 activity (Fig. 3) and these results showed that compounds **14**, **4** and **6** initiated apoptosis at an earlier stage than camptothecin.

Maximal caspase 8 activity was observed in the Caco-2 cells within 4 h of exposure to compounds **3**, **7**, **12** and **13** (Fig. 3); and within 2 h of exposure to compounds **4** (Fig. 3), **6** and **14**. Maximal caspase 3 activity was noted in the Caco-2 cells after 2 h of exposure to compounds **4** (Fig. 3), **6** and **14** and after 4 h of exposure to compound **3**. Caspase 3 activity in Caco-2 cells increased between 2 and 4 h after exposure to compounds **7**, **13** (Fig. 3) and between 2 and 8 h after exposure to compound **12**. The effects of these imidazopyridines on caspase 8 and caspase 3 activities in Caco-2 cells produced similar effects to that observed in the HT-29 cells. As before, the high levels of caspase 3 activity shows that apoptosis was initiated shortly after exposure to the imidazo[1,2-*a*]pyridines.

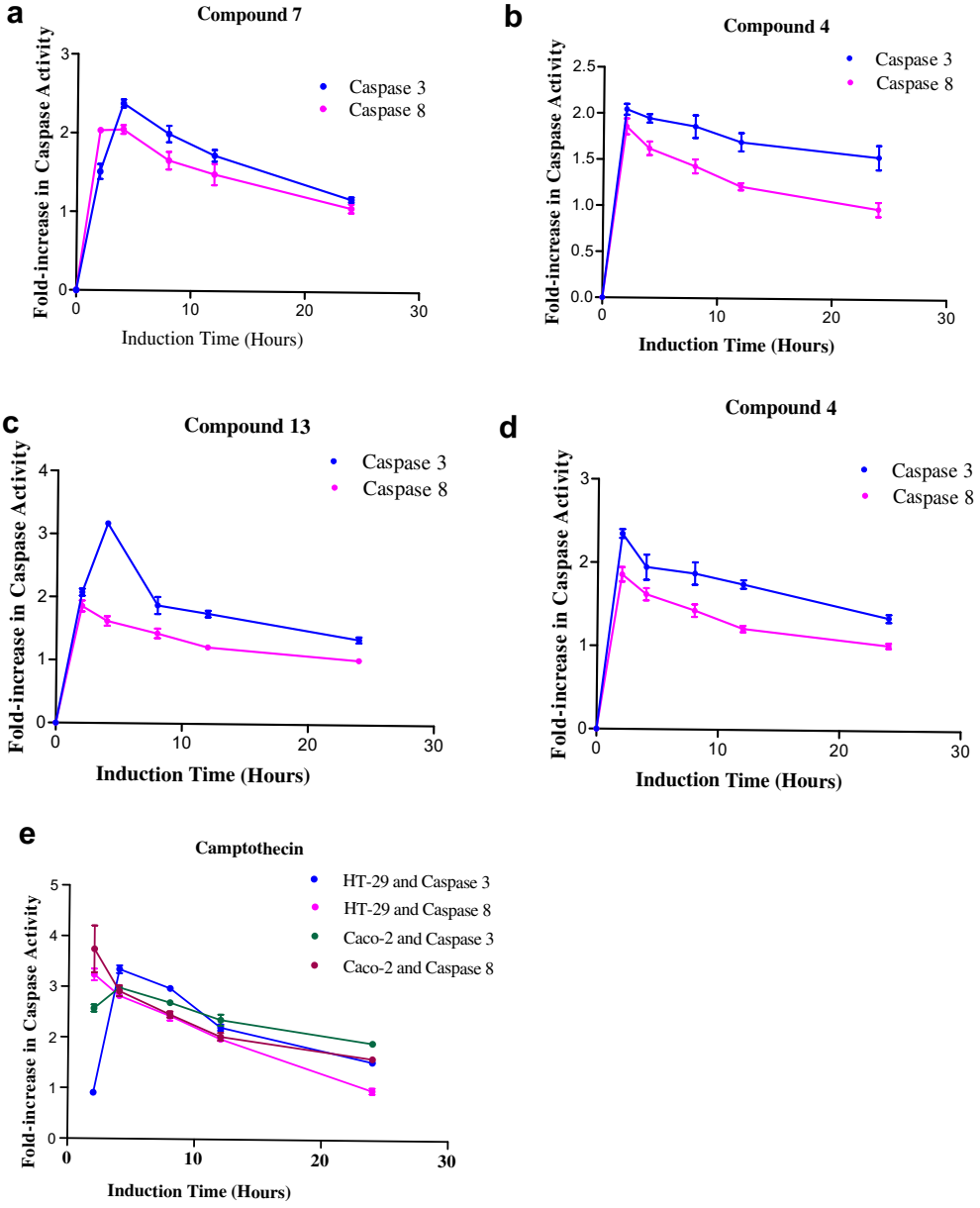

Fig. 3. Time-dependent induction of caspase 3 and caspase 8 activity by (a) compound **7** in HT-29 cells, (b) compound **4** in HT-29 cells, (c) compound **13** in Caco-2 cells, (d) compound **4** in Caco-2 cells and (e) camptothecin in HT-29 and Caco-2 cells. Each point represents the mean and standard deviation of the triplicate values of caspase 3 and caspase 8 activity after cell exposure to the selected compounds over 2 h, 4 h, 8 h, 12 h and 24 h.

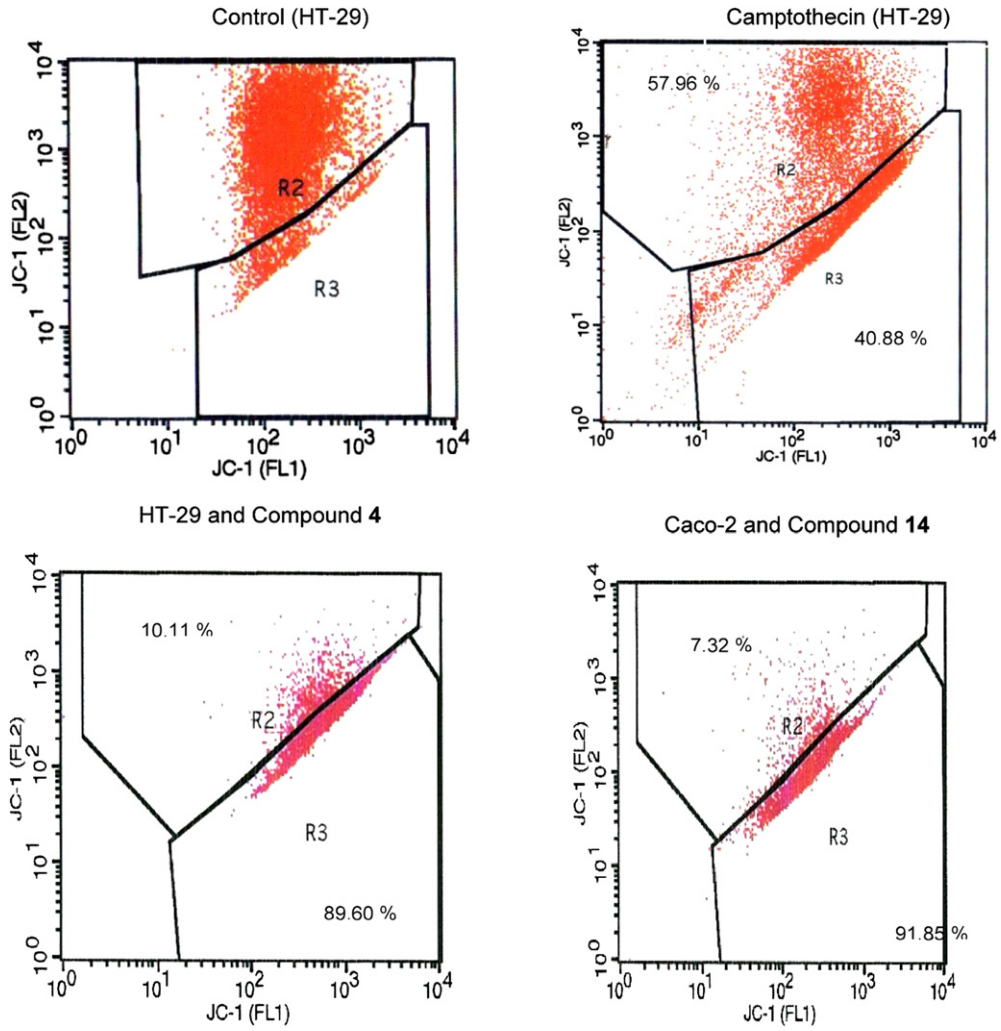

Fig. 4. JC-1 staining in control and apoptotic cells induced by camptothecin, compounds **4**, and **14**.

Camptothecin was also tested in these caspase induction studies and the results are shown in Fig. 3.

2.2.5. Effects on the mitochondrial membrane potential ($\Delta\psi_m$)

There is increasing evidence that altered mitochondrial function is linked to apoptosis. In particular, a decreasing mitochondrial transmembrane potential is associated with mitochondrial dysfunction [5] and has been shown to be a vital factor in controlling the induction of apoptosis. Loss of mitochondrial membrane potential, $\Delta\psi_m$, occurs early in the apoptotic process. The $\Delta\psi_m$ results from the asymmetrical distribution of protons on both sides of the inner mitochondrial membrane, giving rise to a chemical (pH) and electrical gradient, which is essential for mitochondrial function. The collapse of the $\Delta\psi_m$ during apoptosis was noticed in several studies and it has thus been suggested that the depolarisation of the mitochondria is one of the first events which occurs in apoptosis and could be a prerequisite for the release of cytochrome *c*. Since the collapse of the $\Delta\psi_m$ does not always occur in apoptosis, the depolarisation of the $\Delta\psi_m$ may only be a cause of, or associated with apoptosis in some systems. To assess whether disruption of the $\Delta\psi_m$ was involved in the apoptotic action of the imidazo[1,2-*a*]pyridines in this study, the cationic fluorescent dye 5,5′,6,6′-tetrachloro-1,1′,3,3′-tetraethylbenzimidazolcarbocyanine iodide (JC-1)-based flow cytometry Mitochondrial Membrane Potential Detection kit (BD Biosciences) was used to measure mitochondrial membrane depolarisation in viable cells.

There was a significant increase in the number of cells with decreased fluorescence, indicative of a change in the $\Delta\psi_m$, in the populations induced to undergo apoptosis. Compound **4** was shown to cause the greatest change in $\Delta\psi_m$ in the HT-29 cells (Fig. 4), with 89.60% of the mitochondria undergoing a change in the $\Delta\psi_m$ in comparison to 10.11% of viable cells remaining after treatment. Compound **14** was observed to cause the greatest loss in the $\Delta\psi_m$ in the Caco-2 cells with an average of 91.85% of cells

Table 5
Analysis of mitochondrial membrane depolarisation induced by the imidazo[1,2-*a*] pyridines in the HT-29 and Caco-2 colon cancer cell lines.

Compound	% cells with depolarized $\Delta\psi_m$	
	HT-29	Caco-2
3	85.92	85.12
4	89.60	83.33
6	63.09	76.10
7	83.33	81.91
12	65.30	78.00
13	79.62	79.17
14	84.29	91.85
Camptothecin	44.00	40.88

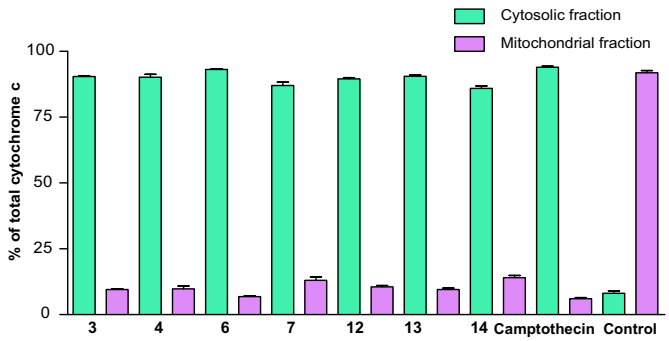

Fig. 5. Cytochrome *c* percentage in the cytosolic and mitochondrial fractions of HT-29 cells after treatment with imidazopyridines **3**, **4**, **6**, **7**, **12**, **13**, **14** and camptothecin for 24 h. The bars represent the mean ± SEM ($n = 3$).

undergoing a change in the $\Delta\psi_m$. These findings suggest that apoptosis induced by the imidazo[1,2-*a*]pyridine derivatives are associated with a depolarisation of the mitochondrial membrane.

The percentages of $\Delta\psi_m$ in the imidazo[1,2-*a*]pyridine-treated HT-29 and Caco-2 cells compared with the control cells are summarized in Table 5.

2.2.6. Effects on the release of cytochrome *c*

Cytochrome *c* is an electron transport protein which is normally located between the inner and outer mitochondrial membranes. Disruption of the $\Delta\psi_m$ results in the opening of the mitochondrial membrane pores, causing the release of soluble intermembrane proteins such as cytochrome *c*, which contributes to caspase 3 activation and subsequently induces apoptosis. To determine whether the observed reduction of $\Delta\psi_m$ by the imidazo[1,2-*a*]pyridines could lead to cytochrome *c* release from the mitochondria into the cytosol, cell lysates were subfractionated and cytosolic and mitochondrial cytochrome *c* levels were determined by a human cytochrome *c* ELISA assay (Assay Designs).

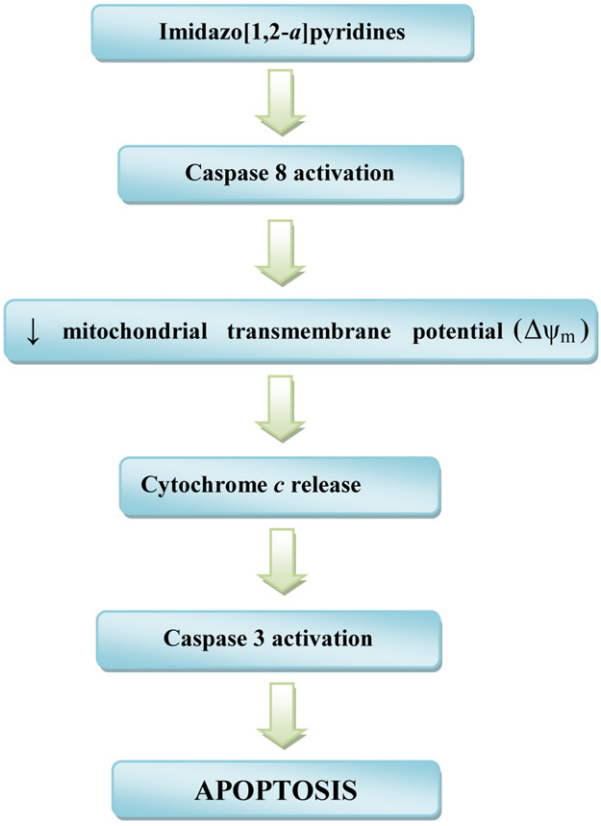

Fig. 6. Proposed mechanism of the imidazo[1,2-*a*]pyridine-induced apoptosis in the HT-29 and Caco-2 cell lines.

Consistent with the loss of $\Delta\psi_m$, cytochrome *c* release into the cytosol was clearly identified after exposure to the novel compounds for 24 h, with cytochrome *c* levels significantly higher ($p = 0.00001$) in the cytosolic fraction than the mitochondrial fractions of the treated cells, whilst cytochrome *c* remained concentrated in the mitochondria in the untreated cells (Fig. 5). This demonstrated that the compounds induced the loss of $\Delta\psi_m$ accompanied with increased levels of cytochrome *c* in the cytosol of both the HT-29 (Fig. 5) and Caco-2 cells (figure not shown).

The untreated cells had higher cytochrome *c* levels in the mitochondrial fraction of both cell lines than the cytosolic fraction ($p = 0.00001$). These results indicate the translocation of cytochrome *c* from the mitochondria to the cytoplasm after treatment with the selected compounds. This confirms the results obtained with the JC-1 dye (Table 5) which suggests that the mitochondria are implicated in the imidazo[1,2-*a*]pyridine-induced apoptosis.

As a result of these experimental observations, we have demonstrated that the observed imidazo[1,2-*a*]pyridine-induced caspase 8 activation was the upstream event of the mitochondrial cytochrome *c* release, which in turn, led to the activation of caspase 3. It is also suggested that caspase 3 could be activated independent of the mitochondrial cytochrome *c* release, as a downstream event of caspase 8 activation (Fig. 6).

3. Conclusions

The biological properties of the imidazo[1,2-*a*]pyridine class of compounds have received considerable attention in recent years, however their effect on colon cancer cell lines has not yet been established. In the present study, we demonstrated a time- and dose-dependent induction of apoptosis with a series of novel, structurally related 6-substituted imidazo[1,2-*a*]pyridines in HT-29 and Caco-2 colon cancer cells.

Among the selected compounds that were tested against the HT-29 and Caco-2 cell lines, compounds **4** and **7** are significantly cytotoxic ($p < 0.05$) and elicit apoptosis in the cells at very low micromolar concentrations. Importantly, the compounds showed a degree of selective cytotoxicity against the cancer cell lines, with minimal cytotoxicity against white blood cells. The proteolytic phase of apoptosis was initiated 2 h after treatment with these compounds. The imidazo[1,2-*a*]pyridines are also associated with a marked reduction in the $\Delta\psi_m$, as well as causing an increase in cytochrome *c* levels within the cytosolic fraction of the cells. The induction of apoptosis (Fig. 6) is considered to be the main mechanism underlying the therapeutic efficacy of anticancer drugs, hence the present results suggest that the imidazo[1,2-*a*]pyridines described here may successfully be developed into novel chemotherapeutic drugs for the treatment of colon cancer.

4. Experimental procedures

4.1. Chemistry

4.1.1. General experimental procedures

^{1}H NMR and ^{13}C NMR spectra were recorded on a Bruker AVANCE 300 spectrometer. All spectra were recorded in $CDCl_3$, MeOD or d6DMSO. All chemical shift values are reported in parts per million referenced against TMS which is given an assignment of zero parts per million. Coupling constants (J-values) are given in

Hertz (Hz). Infrared spectra were recorded on a Bruker Tensor 27 standard system spectrometer. Macherey–Nagel Kieselgel 60 (particle size 0.063–0.200 mm) was used for conventional silica gel column chromatography with various EtOAc and hexane mixtures as the mobile phase. TLC was performed on aluminium-backed Macherey–Nagel Alugram Sil G/UV254 plates pre-coated with 0.25 mm silica gel 60. HPLC purity of compounds synthesized was determined using a phenomenex Luna 5u C18 column using an acetonitrile/water mixture. All compounds were >95% pure by this HPLC method. Microwave reactions were carried out on a commercial CEM Discover microwave oven.

4.1.1.1. 4-[3-(2,6-Dimethyl-phenylamino)-6-nitroimidazo[1,2-a]pyridin-2-yl]-benzene-1,3-diol ***1***. 2-Amino-5-nitropyridine (0.4601 g, 3.31 mmol) was dissolved in 1,4-dioxane (5 mL) 2,4-Dihydroxybenzaldehyde (0.4426 g, 3.20 mmol), 2,6-dimethylphenyl isocyanide (0.4157 g, 3.17 mmol), K10 (0.4175 g) and a stirrer bar were added to the flask with further 1,4-dioxane (5 mL). The reaction was refluxed for 72 h at 110 °C while monitoring the reaction progress with TLC. The K10 was filtered-off using boiling hot EtOAc. The filtrate was collected and the solvent removed *in vacuo* before further drying on the high-vacuum line to yield a red-brown solid. The solid was dissolved in dichloromethane and on cooling a red powder settled out and was collected and was then recrystallised with EtOAc to reveal a red powder **1** (0.1344 g, 11%). **Mp** = 288–293 °C (EtOAc); **IR** = ν_{max} (cm^{-1}) = 3427, 3365, 3111, 2917, 1697, 1593, 1568, 1540, 1472, 1443, 1373, 1352; ^{1}**H NMR** (300 MHz, DMSO) δ 12.28 (s, 1H), 9.65 (s, 1H), 9.02 (s, 1H), 8.03 (d, J = 8.7, 1H), 7.84 (d, J = 9.2, 1H), 7.50 (d, J = 8.1, 1H), 7.42 (s, 1H), 6.97 (d, J = 6.2, 2H), 6.77 (t, J = 6.9, 1H), 6.30 (s, 1H), 6.15 (d, J = 7.1, 1H), 1.93 (s, 6H); ^{13}**C NMR** (75 MHz, DMSO) δ 159.1, 158.3, 139.6, 138.4, 137.0, 134.9, 129.5, 128.6, 126.6, 122.7, 122.1, 121.3, 118.7, 115.4, 107.4, 106.8, 103.0, 18.3; **HRMS** (m/z) calculated for $C_{21}H_{19}N_4O_4$, (M + H), 391.1406, found 391.1389.

4.1.1.2. 4-[6-Bromo-3-(2,6-dimethyl-phenylamino)-imidazo[1,2-a]pyridin-2-yl]-benzene-1,3-diol ***2***. 2-Amino-5-bromopyridine (0.2895 g, 1.67 mmol) was dissolved in 1,4-dioxane (5 mL) in a small round-bottomed flask. 2,4-dihydroxybenzaldehyde (0.2708 g, 1.96 mmol), 2,6-dimethylphenyl isocyanide (0.2782 g, 2.12 mmol), K10 (0.3365 g) was added to the flask with further 1,4-dioxane (5 mL). The reaction was refluxed for 80 h at 110 °C and then worked up as previously described to afford a yellow-brown solid. The solid was dissolved in methanol and the yellow solid of **2** that crystallized to the bottom of the flask was collected (0.5258 g, 74%). **Mp** = 265–270 °C; **IR** = ν_{max} (cm^{-1}) = 3593, 3337, 2920, 1595, 1500, 1473, 1452, 1403, 1329; ^{1}**H NMR** (300 MHz, MeOD) δ 7.95 (d, J = 1.0, 1H), 7.65 (d, J = 8.6, 1H), 7.49 (d, J = 9.4, 1H), 7.36 (dd, J = 9.4, 1.8, 1H), 6.94 (d, J = 7.4, 2H), 6.75 (t, J = 7.5, 1H), 6.32 (d, J = 2.4, 1H), 6.18 (dd, J = 8.6, 2.4, 1H), 1.94 (s, 6H); ^{13}**C NMR** (75 MHz, MeOD) δ 159.9, 159.7, 141.5, 138.8, 138.2, 130.7, 129.9, 129.0, 127.2, 123.7, 122.2, 121.8, 117.6, 110.0, 108.3, 107.8, 104.0, 18.7, 18.7; **HRMS** (m/z) calculated for $C_{21}H_{19}BrN_3O_2$, (M + H), 424.0661, found 424.0645.

4.1.1.3. [2-(3,4-Dimethoxy-phenyl)-6-methyl-imidazo[1,2-a]pyridin-3-yl]-(2,6-dimethylphenyl)-amine ***3***. 2-Amino-5-methylpyridine (0.2630 g, 2.23 mmol) was dissolved in 1,4-dioxane (3 mL) in a small round-bottomed flask. 3,4-dimethoxybenzaldehyde (0.5555 g, 3.34 mmol), 2,6-dimethylphenyl isocyanide (0.3544 g, 2.70 mmol), K10 (0.2609 g) were added to the flask with further 1,4-dioxane (3 mL). The reaction was refluxed for 8 h at 110 °C and stirred for a further 88 h at rt, the reaction was then stopped and worked-up as previously described to yield a brown oil. The oil was purified by silica gel column chromatography (80% EtOAc/hexane) to afford an off-white/pink powder of **3** in 42% yield (0.3620 g). **Mp** = 185–188 °C; **IR** = ν_{max} (cm^{-1}) = 3370, 3345, 2959, 1587, 1509, 1465, 1409, 1372, 1333, 1300; ^{1}**H NMR** (300 MHz, $CDCl_3$) δ 7.64 (dd, J = 8.4, 1.9, 1H), 7.60 (s, 1H), 7.50 (d, J = 9.2, 1H), 7.47 (d, J = 1.9, 1H), 7.01 (dd, J = 9.2, 1.5, 1H), 6.96 (d, J = 7.5, 2H), 6.82 (d, J = 8.5, 1H), 6.77 (t, J = 7.5, 1H), 5.56 (br s, 1H), 3.87 (s, 3H), 3.73 (s, 3H), 2.26 (s, 3H), 2.00 (s, 6H); ^{13}**C NMR** (75 MHz, $CDCl_3$) δ 149.0, 148.7, 141.0, 140.2, 137.7, 130.2, 128.0, 126.3, 124.7, 122.4, 120.7, 120.2, 119.8, 119.5, 116.4, 111.1, 110.0, 55.9, 55.8, 18.7, 18.6; **HRMS** (m/z) calculated for $C_{24}H_{26}N_3O_2$, (M + H), 388.2025, found 388.2023.

4.1.1.4. Benzyl-[6-bromo-2-(2,5-dimethoxy-phenyl)-imidazo[1,2-a]pyridin-3-yl]-amine ***4***. 2-Amino-5-bromopyridine (0.3026 g, 1.75 mmol) was dissolved in 1,4-dioxane (5 mL) in a small round-bottomed flask. 2,5-dimethoxybenzaldehyde (0.2975 g, 1.79 mmol), Benzyl isocyanide (0.1500 g, 1.28 mmol), K10 (0.3194 g) were added to the flask with further 1,4-dioxane (5 mL). The reaction was refluxed for 72 h at 110 °C and after work-up as previously described yielded a brown oil. The oil was purified by silica gel column chromatography (50% EtOAc/hexane) to give the product **4** as a yellow oil (0.3760 g, 67%). **IR** = ν_{max} (cm^{-1}) = 3339, 2933, 2832, 1586, 1559, 1496, 1453, 1419, 1387, 1322; ^{1}**H NMR** (300 MHz, $CDCl_3$) δ 8.19 (d, J = 1.1, 1H), 7.53 (d, J = 9.4, 1H), 7.23–7.12 (m, 5H), 7.09–7.02 (m, 2H), 6.88 (d, J = 1.5, 2H), 4.42 (br s, 1H), 3.92 (d, J = 5.3, 2H), 3.83 (s, 3H), 3.75 (s, 3H); ^{13}**C NMR** (75 MHz, $CDCl_3$) δ 154.3, 150.2, 140.0, 139.0, 134.0, 128.4, 128.2, 128.0, 127.4, 126.9, 124.0, 122.6, 118.0, 115.6, 113.6, 106.6, 57.2, 55.9, 52.4; **HRMS** (m/z) calculated for $C_{22}H_{21}BrN_3O_2$, (M + H), 388.0817, found 438.0806.

4.1.1.5. 2-(-3,4-bis(Benzyloxy)phenyl)-6-bromo-N-cyclohexylimidazo[1,2-a]pyridine-3-amine ***5***. 2-Amino-5-bromopyridine (0.200 g, 1.156 mmol) was dissolved in dioxane (5 mL). 3,4-Dibenzyloxybenzaldehyde (0.0405 g, 1.27 mmol), K10 (0.210 g) and cyclohexyl isocyanide (0.129 g, 1.171 mmol) was added to the mixture, together with more dioxane (3 mL). The mixture was stirred at reflux for 6 h and then at rt for 18 h. The product **5** crystallized in the reaction flash and was recrystallised from EtOAc to afford **5** (0.295 g) as a yellow solid in a yield of 44%. **Mp** = 188–190 °C; **IR** = ν_{max} (cm^{-1}) = 2920, 1580, 1504, 1436, 1403, 1318; ^{1}**H NMR** (300 MHz, $CDCl_3$) δ 8.24 (s, 1H), 7.72 (d, J = 1.7, 1H), 7.57–7.42 (m, 6H), 7.42–7.28 (m, 6H), 7.18 (dd, J = 9.4, 1.7, 1H), 7.00 (d, J = 8.4, 1H), 5.28 (s, 2H), 5.20 (s, 2H), 3.31 (br s, 1H), 2.91 (s, 1H), 1.81–1.53 (m, 5H), 1.27–1.08 (m, 5H); ^{13}**C NMR** (75 MHz, $CDCl_3$) δ 149.3, 148.9, 139.6, 137.5, 137.4, 137.1, 128.6, 128.6, 127.9, 127.5, 124.7, 123.0, 120.5, 117.7, 115.1, 114.0, 106.8, 71.4, 71.4, 56.9, 34.2, 25.8, 24.9; **HRMS** (m/z) calculated for $C_{33}H_{33}BrN_3O_2$, (M + H), 582.1756, found 582.1730.

4.1.1.6. [6-Bromo-2-(3,4-dimethoxy-phenyl)-imidazo[1,2-a]pyridin-3-yl]-(2,6-dimethylphenyl)-amine ***6***. 2-Amino-5-bromopyridine (0.3900 g, 2.25 mmol) was dissolved in 1,4-dioxane (3 mL) in a small round-bottomed flask. 3,4-dimethoxybenzaldehyde (0.3927 g, 2.36 mmol), 2,6-dimethylphenyl isocyanide (0.3108 g, 2.37 mmol), K10 (0.3707 g) were added to the flask with further 1,4-dioxane (3 mL). The reaction was refluxed for 6 h at 110 °C and stirred for a further 92 h at rt. After work-up of the reaction, as described above, a brown solid was obtained. The solid was dissolved in methanol and on cooling yielded a yellow solid which was filtered and collected. The product **6** a yellow, crystalline material was obtained by re-crystallization (CH_2Cl_2/hexane) in a yield of 67% (0.6944 g). **Mp** = 208–210 °C (CH_2Cl_2/hexane); **IR** ν_{max} (cm^{-1}) = 3361, 2960, 1687, 1623, 1584, 1505, 1469, 1411, 1356, 1326; ^{1}**H NMR** (300 MHz, $CDCl_3$) δ 7.94 (d, J = 0.9, 1H), 7.58 (dd, J = 8.4, 1.9, 1H), 7.48 (d, J = 9.4, 1H), 7.44 (d, J = 1.8, 1H), 7.21 (dd, J = 9.4, 1.7, 1H), 6.98 (d, J = 7.5, 2H), 6.85–6.75 (m, 2H), 5.50 (br s, 1H), 3.88 (s, 3H), 3.72 (s, 3H), 2.00 (s, 6H); ^{13}**C NMR** (75 MHz,

$CDCl_3$): δ 149.0, 149.0, 140.5, 139.7, 139.0, 130.3, 128.0, 125.8, 124.8, 122.6, 121.1, 120.0, 119.9, 117.8, 111.0, 110.0, 107.3, 55.9, 55.7, 18.7, 18.6; **HRMS** (*m*/*z*) calculated for $C_{23}H_{22}BrN_3O_2$, (M + H), 452.0974, found 452.0975.

4.1.1.7. 2-(2,4-bis(Benzyloxy)phenyl)-3-(cyclohexylamino)imidazo[1,2-a]pyridine-6-carboxamide ***7***. 6-Aminonicotinamide (0.500 g, 3.64 mmol), 2,4-bis(benzyloxy)benzaldehyde (1.160 g, 3.64 mmol), cyclohexyl isocyanide (0.398 g, 3.64 mmol) and K10 (0.50 g) was dissolved in 1,4-dioxane (20 mL) at rt. The reaction mixture was refluxed for 40 h at 110 °C while monitoring the reaction progress with TLC. After work-up of the reaction as described previously, the residue obtained was subjected column chromatography on silica gel (ethyl acetate) to furnish a yellow compound which was crystallized from hexane to give pure desired product 2-(2,4-bis(benzyloxy)phenyl)-3-(cyclohexylamino)imidazo[1,2-*a*]pyridine-6-carboxamide **7** (1.70 g, 85%) as a yellow solid. **Mp** = 112–115 °C; **IR** ν_{max} (cm^{-1}) = 2924, 1667, 1607, 1504, 1452, 1366; ^{1}**H NMR** (300 MHz, $CDCl_3$) δ 8.75 (s, 1H), 7.80 (d, *J* = 9.1, 1H), 7.49–7.27 (m, 12H), 6.81–6.72 (m, 2H), 6.52 (br s, 1H), 5.08 (s, 2H), 5.05 (s, 2H), 3.88 (d, *J* = 8.1, 1H), 2.71–2.55 (m, 1H), 1.68–1.40 (m, 5H), 1.13–0.83 (m, 5H); ^{13}**C NMR** (75 MHz, $CDCl_3$) δ 167.8, 159.9, 156.2, 141.7, 136.7, 136.0, 135.0, 132.6, 128.8, 128.7, 128.5, 128.2, 127.8, 127.7, 124.9, 121.6, 118.3, 117.2, 116.4, 107.4, 101.6, 71.7, 70.3, 56.6, 34.0, 25.7, 24.8; HRMS (*m*/*z*) calculated for $C_{34}H_{35}N_4O_3$, (M + H), 547.2709, found 547.2707.

4.1.1.8. 2-(3,4-bis(Benzyloxy)phenyl)-N-cyclohexyl-6-nitroimidazo[1,2-a]prridin-3-amine ***8***. Amino-5-nitropyridine (0.3714 g, 2.700 mmol), 2,4-dibenzyloxybenzaldehyde (0.8628 g, 2.710 mmol), cyclohexyl isocyanide (0. 2988 g, 2.712 mmol) and K10 (0.37 g) was dissolved in 1,4-dioxane (18 mL). The reaction mixture was refluxed for 25 h at 105 °C. The reaction mixture was worked-up as previously described and was subjected column chromatography on silica gel (30% EtOAc/hexane) to give the desired product **10** (0.6298 g, 43%) as a orange solid. **Mp** = 175–178 °C; **IR** ν_{max} (cm^{-1}) = 2924, 2852, 1631, 1584, 1537, 1508, 1435, 1347, 1320; ^{1}**H NMR** (300 MHz, $CDCl_3$) δ 9.21 (d, *J* = 1.8, 1H), 7.89 (dd, *J* = 9.8, 2.2, 1H), 7.73 (d, *J* = 1.8, 1H), 7.64–7.43 (m, 6H), 7.42–7.29 (m, 6H), 7.01 (d, *J* = 8.4, 1H), 5.28 (s, 2H), 5.21 (s, 2H), 3.48 (br s, 1H), 3.03–2.90 (m, 1H), 1.80–1.55 (m, 5H), 1.29–1.07 (m, 5H); ^{13}**C NMR** (75 MHz, $CDCl_3$) δ 149.5, 149.3, 141.0, 139.5, 137.3, 137.1, 128.7, 128.7, 128.0, 127.5, 127.5, 126.4, 126.2, 123.1, 120.7, 118.6, 116.4, 115.0, 114.1, 71.5, 71.3, 57.2, 34.2, 25.6, 24.9; **HRMS** (*m*/*z*) calculated for $C_{33}H_{33}N_4O_4$, (M + H), 549.2502, found 549.2506.

4.1.1.9. 4-(3-(2,6-Dimethyl-phenylamino)imidazo[1,2-a]pyridine-2-yl) benzene-1,3-diol ***9***. Aminopyridine (0.4270 g, 4.537 mmol), 2,4-dihydroxybenzaldehyde (0.62811 g, 4.548 mmol), 2,6-dimethylphenyl isocyanide (0.60110 g, 4.547 mmol) and K 10 (0.42 g) was dissolved in 1,4-dioxane (15 mL) at room temperature. The reaction mixture was refluxed for 10 h at 110 °C. The mixture was worked up as previously described to afford residue was subjected to silica gel column chromatography (30% EtOAc/hexane) which afforded a light brown/yellow compound which was crystallized from hexane to give pure desired product **9** (0.2977 g, 19%) as a yellow solid. **Mp** = 245–250 °C; **IR** ν_{max} (cm^{-1}) = 3348, 2917, 1596, 1524, 1503, 1472, 1447, 1390, 1343, 1301; ^{1}**H NMR** (300 MHz, MeOD) δ 7.82 (d, *J* = 6.9, 1H), 7.76 (d, *J* = 8.6, 1H), 7.54 (d, *J* = 9.0, 1H), 7.34–7.24 (m, 1H), 6.89 (dd, *J* = 13.0, 7.1, 3H), 6.71 (t, *J* = 7.5, 1H), 6.34 (d, *J* = 2.4, 1H), 6.21 (dd, *J* = 8.6, 2.4, 1H), 1.94 (s, 6H); ^{13}**C NMR** (75 MHz, MeOD) δ 159.7, 159.7, 142.0, 140.4, 137.5, 130.7, 129.9, 126.9, 126.2, 123.6, 121.8, 121.3, 116.8, 113.8, 110.4, 107.7, 104.0, 18.8, 18.7; (ESI negative) **HRMS** (*m*/*z*) calculated for $C_{21}H_{18}N_3O_2$, (M − H), 344.1399, found 344.1403.

4.1.1.10. 4-(3-(Cyclohexylamino)imidazo[1,2-a]pyridine-2-yl)benzene-1,3-diol ***10***. Aminopyridine (0.4812 g, 5.113 mmol), 2,4-dihydroxybenzaldehyde (0.7768 g, 5.624 mmol), cyclohexyl isocyanide (0.6194 g, 5.622 mmol) and K 10 (0.48 g) was dissolved in 1,4-dioxane (20 mL). The reaction mixture was refluxed for 30 h at 105 °C. The reaction mixture was worked-up as previously described and was subjected column chromatography on silica gel (50% EtOAc/hexane) to give the desired product **10** (0.2480 g, 15%) as a yellow solid. **Mp** = 195–200 °C; **IR** ν_{max} (cm^{-1}) = 3040, 2929, 2853, 2625, 1618, 1589, 1497, 1449, 1385, 1357, 1328, 1315; ^{1}**H NMR** (300 MHz, MeOD) δ 8.29 (d, *J* = 6.8, 1H), 7.81 (d, *J* = 8.5, 1H), 7.49 (d, *J* = 9.0, 1H), 7.35–7.26 (m, 1H), 6.97 (t, *J* = 6.8, 1H), 6.44 (dd, *J* = 8.5, 2.4, 1H), 6.39 (d, *J* = 2.4, 1H), 2.94–2.82 (m, 1H), 1.81–1.49 (m, 6H), 1.29–1.10 (m, 5H); ^{13}**C NMR** (75 MHz, MeOD) δ 160.1, 157.9, 142.3, 140.0, 136.4, 131.1, 126.5, 124.1, 116.6, 113.6, 112.2, 108.6, 104.6, 58.1, 34.4, 26.8, 25.9; (ESI negative) **HRMS** (*m*/*z*) calculated for $C_{19}H_{20}N_3O_2$, (M − H), 322.1556, found 322.1556.

4.1.1.11. 2-(2,4-Dimethoxyphenyl)-N-(2,6-dimethylphenyl)-6-nitroimidazo[1,2-a]pyridine-3-amine ***11***. 2-Amino-5-nitropyridine (0.3010 g, 2.1637 mmol), 2,4-dimethoxybenzaldehyde (0.3955 g, 2.380 mmol), 2,6-dimethylphenyl isocyanide (0.3148 g, 2.3815 mmol) and K 10 (0.30 g) was dissolved in 1,4-dioxane (20 mL) at room temperature. The reaction mixture was refluxed for 24 h at 110 °C. After work-up as described previously the residue was subjected column chromatography on silica gel (30% EtOAc/hexane) to give pure desired product, 2-(2,4-dimethoxyphenyl)-*N*-(2,6-dimethylphenyl)-6-nitroimidazo[1,2-*a*]pyridine-3-amine **11** (0.5832 g, 68%) as a yellow solid. **Mp** = 172–176 °C; **IR** ν_{max} (cm^{-1}) = 2926, 2847, 2660, 1636, 1615, 1575, 1535, 1451, 1429, 1387, 1348; ^{1}**H NMR** (300 MHz, $CDCl_3$) δ 8.61 (s, 1H), 7.93 (s, 1H), 7.86 (dd, *J* = 9.7, 1.8, 1H), 7.71 (d, *J* = 8.6, 1H), 6.97 (d, *J* = 7.4, 2H), 6.88 (dd, *J* = 8.3, 6.5, 1H), 6.62 (dd, *J* = 8.6, 2.2, 1H), 6.52 (d, *J* = 2.2, 1H), 6.47 (s, 1H), 3.93 (s, 3H), 3.85 (s, 3H), 1.97 (s, 6H); ^{13}**C NMR** (75 MHz, $CDCl_3$) δ 161.7, 157.5, 140.1, 138.1, 137.0, 135.1, 135.1, 132.0, 129.7, 128.4, 126.0, 123.2, 122.3, 116.9, 116.8, 114.8, 106.0, 99.2, 99.2, 56.2, 55.7, 18.5, 18.5; **HRMS** (*m*/*z*) calculated for $C_{23}H_{23}N_4O_4$, (M + H), 419.1719, found 419.1736.

4.1.1.12. 6-Bromo-2(2,4-dimethoxyphenyl)-N-(2,6-dimethylphenyl) imidazo[1,2-a]pyridine-3-amine ***12***. 2-Amino-5-bromopyridine (0.5031 g, 2.88 mmol), 2,4-dimethoxybenzaldehyde (0.4802 g, 2.88 mmol), 2,6-dimethylphenyl isocyanide (0.3790 g, 2.88 mmol) and K10 (0.50 g) was dissolved in 1,4-dioxane (20 mL) at room temperature. The reaction mixture was refluxed for 30 h at 110 °C. After work-up as described previously, the residue was subjected column chromatography on silica gel (30% EtOAc/hexane) that afforded a light brown/yellow compound which was crystallized from hexane to give pure desired product **12** (1.104 g, 84%) as a yellow solid. **Mp** = 159–163 °C; **IR** ν_{max} (cm^{-1}) = 3288, 1655, 1613, 1568, 1518, 1473, 1439, 1404, 1326, 1302; ^{1}**H NMR** (300 MHz, $CDCl_3$) δ 7.56 (d, *J* = 8.4, 2H), 7.44 (d, *J* = 9.4, 1H), 7.10 (dd, *J* = 9.4, 1.7, 1H), 6.90 (d, *J* = 7.4, 2H), 6.80–6.71 (m, 1H), 6.58 (dd, *J* = 8.5, 2.2, 1H), 6.49 (d, *J* = 2.1, 1H), 5.96 (s, 1H), 3.84 (s, 3H), 3.81 (s, 3H), 1.89 (s, 6H); ^{13}**C NMR** (75 MHz, $CDCl_3$) δ 161.1, 157.4, 139.2, 139.1, 134.3, 131.9, 129.4, 127.0, 126.0, 123.7, 122.0, 121.7, 118.1, 115.9, 106.6, 105.6, 99.0, 99.0, 55.9, 55.5, 18.3, 18.3; **HRMS** (*m*/*z*) calculated for $C_{23}H_{23}BrN_3O_2$, (M + H), 452.0974, found 452.0963.

4.1.1.13. 2-(2,4-Dimethoxyphenyl)-N-(2,6-dimethlyphenyl)-6-nitroimidazo[1,2-a]pyridine-3-amine ***13***. 2-Amino-5-methylpyridine (0.500 g, 4.62 mmol), 2,4-dimethoxybenzaldehyde (0.768 g, 4.62 mmol), 2,6-dimethylphenyl isocyanide (0.606 g, 4.62 mmol) and K10 (0.5 g) was dissolved in 1,4-dioxane (20 mL) at room temperature. The reaction mixture was refluxed for 48 h at 110 °C. The residue after work-up was

subjected column chromatography on silica gel (50% EtOAc/hexane) affording a brown pasty compound which was crystallized from hexane to give pure desired product **13** as a light brown solid (1.502 g, 84%). **Mp** = 137–140 °C; **IR** ν_{max} (cm^{-1}) = 3201, 3001, 2922, 2833, 1596, 1582, 1532, 1467, 1449, 1436, 1411, 1395; **^{1}H NMR** (300 MHz, $CDCl_3$) δ 7.57 (d, J = 8.4, 1H), 7.45 (d, J = 9.1, 1H), 6.88 (dd, J = 15.5, 4.4, 3H), 6.74–6.65 (m, 1H), 6.56 (dd, J = 8.5, 2.2, 1H), 6.47 (d, J = 2.2, 1H), 5.88 (s, 1H), 3.80 (s, 3H), 3.78 (s, 3H), 2.15 (d, J = 6.7, 3H), 1.87 (s, 6H); **^{13}C NMR** (75 MHz, $CDCl_3$) δ 160.8, 157.4, 140.1, 139.9, 133.6, 131.8, 129.3, 126.4, 126.0, 122.8, 121.3, 120.9, 119.7, 116.8, 116.5, 105.4, 98.9, 55.8, 55.5, 18.5, 18.3, 18.3; **HRMS** (m/z) calculated for $C_{24}H_{26}N_3O_2$, (M + H), 388.2025, found 388.2025.

*4.1.1.14. [2-(3,4-Dimethoxy-phenyl)-6-phenyl-imidazo[1,2-a]pyridin-3-yl]-(2,6-dimethyl-phenyl)-amine **14**.* 6-Bromo-2-(3,4-dimethoxyphenyl)-*N*-(2,6-dimethylphenyl)imidazo[1,2-*a*]pyridin-3-amine **6** (0.25 g, 0.55 mmol), phenylboronic acid (0.101 g, 0.82 mmol), $Pd(PPh_3)_4$ (0.064 g, 10 mol%) and CsF (0.209 g, 1.38 mmol) was dissolved in DME (3 mL) in microwave tube under argon. The reaction mixture was irradiated in a Discovery microwave at 150 °C and 150 W for 20 min. The reaction was concentrated and subjected to column chromatography on silica gel (30–50% EtOAc/hexane) to give desired product **14** (0.188 g, 95%) as a crimson red solid. **Mp** = 158–160 °C (methanol); **IR** ν_{max} (cm^{-1}) = 2929, 1636, 1587, 1509, 1470, 1408; **^{1}H NMR** (300 MHz, $CDCl_3$) δ 7.86 (s, 1H), 7.60 (dd, J = 18.7, 8.6, 2H), 7.42 (d, J = 23.3, 6H), 6.96 (d, J = 7.1, 2H), 6.76 (d, J = 8.0, 2H), 5.50 (s, 1H), 3.78 (s, 3H), 3.69 (s, 3H), 2.01 (s, 6H); **^{13}C NMR** (75 MHz, $CDCl_3$) δ 148.8, 148.6, 140.9, 140.7, 138.7, 137.3, 130.1, 129.1, 127.7, 126.7, 126.5, 126.3, 124.9, 124.7, 120.8, 120.1, 119.7, 119.4, 116.9, 110.9, 109.9, 55.7, 55.6, 18.6, 18.6; **HRMS** (m/z) calculated for $C_{29}H_{28}N_3O_2$, (M + H), 450.2182, found 450.2185.

4.2. Biological cell lines

The study made use of two colonic carcinoma cell lines, namely the HT-29 and Caco-2 (Highveld Biological, South Africa). The cells were maintained in Dulbecco's Modified Eagles Medium (DMEM) (Highveld Biological, South Africa) supplemented with 5% heat-inactivated foetal bovine serum (FBS), and incubated at 37 °C in a CO_2 humidified incubator.

Camptothecin is a S-phase-specific anticancer agent that inhibits the activity of the enzyme DNA topoisomerase 1. It was used as a positive control in the study as several studies have shown the effectivity of camptothecin to induce apoptosis in a dose-dependent manner *in vitro* [23].

4.3. Determining cell viability via the MTT assay

The 3-(4,5-dimethylthiazol-2-yl)-2,5-diphenyltetrazolium bromide (MTT) assay [24] was used to determine cell viability of the two cell lines on exposure to the derivatives for 24 h. The cells were seeded at a density of 30 000 cells/well. Formazan crystals were dissolved in 200 μl DMSO. The absorbance was read at 540 nm using the Absorbance Labsystems Multiskan MS, version 2.4. Compounds showing cytotoxicity at a concentration of 100 μM were further diluted to obtain an IC_{50} concentration. All tests were performed in triplicate.

4.4. Collection of whole blood and isolation of white blood cells from humans

The isolation of human peripheral white blood cells (WBC) was adapted from the Versagene Blood DNA Kit according to the manufacturer's protocol (Gentra Systems). Ethics clearance no: M070519, University of the Witwatersrand.

4.5. Assessment of apoptosis

4.5.1. Annexin V

One of the most important stages of apoptosis involves the attainment of surface changes by dying cells that would eventually result in phagocytosis. Many studies have shown that cells undergoing apoptosis lose the phospholipid asymmetry of their plasma membrane and expose PS, which is translocated to the outer layer of the membrane. Annexin V is a useful tool in detecting apoptotic cells since it binds preferentially to negatively charged phospholipids such as PS. The translocation of PS occurs in both necrosis and apoptosis; hence Annexin V is combined with propidium iodide (PI). The cell staining was assessed using fluorescein isothiocyanate (FITC)-labelled Annexin V (green fluorescence) as well as dye exclusion of PI (negative for red fluorescence). It is possible to detect and quantitate the apoptotic cells on a single-cell basis by flow cytometry and to identify the intact cells (FITC-PI-), early apoptotic (FITC+PI-), late apoptotic or necrotic cells (FITC + PI) [21]. The Annexin V-FITC apoptosis detection kit (BD Biosciences) was used to determine whether apoptosis induction had occurred. The cells were analysed by FACS flow cytometry (BD LSR II flow cytometer) and the data displayed as a two-colour dot plot with FITC-Annexin V (green fluorescence, *X* axis) vs. PI (red fluorescence, *Y* axis).

4.5.2. Colorimetric assay for caspase detection

The activation of caspases initiates apoptosis in mammalian cells. Caspase 3 and caspase 8 activity were detected using the CPP32 and FLICE colorimetric assay kits, respectively. Treated cells were lysed, and the cell lysate was then tested for caspase 3 and caspase 8 activity by the addition of a caspase-specific peptide conjugated to the chromophore *p*-nitroaniline (pNA). Time-dependent studies were performed for protease activity by obtaining results 2, 4, 6, 12, and 24 h after treatment with the compounds.

4.5.3. Mitochondrial membrane potential

The fluorescent mitochondrial-specific cationic dye JC-1 was used according to the manufacturer's specification to measure the collapse of the electrochemical gradient across the mitochondrial membrane.

The cells were analysed by flow cytometry using excitation/emission filters of 485/540 nm (green/FL-1); 540/590 nm (red/FL-2).

4.5.4. Detection of the release of cytochrome c determination

A quantitative concentration of cytochrome *c* in the cell lysates was determined by a human cytochrome *c* Titerzyme Enzyme Immunometric Assay. The kit uses a monoclonal antibody specific for cytochrome *c*, a biotinylated detecting antibody and alkaline phosphatase-conjugated streptavidin to provide a colorimetric detection that enables a quantitative determination of cytochrome *c* in the cell lysates. The treated HT-29 and Caco-2 cells were harvested and rinsed with ice-cold phosphate buffered saline (3.2 mM Na_2HPO_4, 0.5 mM KH_2PO_4, 1.3 mM KCl and 135 mM NaCl, pH 7.4). The cytosolic and mitochondrial fractions were isolated according to the protocol provided by the Mitochondria isolation kit (Assay Designs, Inc.)

4.5.5. Statistics

Significant differences between the control and experimental samples were determined using the Prism3 Instat package, using ANOVA, Student-t test. The values are expressed as mean ± standard error of the mean. Significance was set at a confidence interval of 95% ($p < 0.05$).

Acknowledgements

This work was supported by the National Research Foundation, Pretoria, (NRF, GUN 2053652 and IRDP of the NRF (South Africa) for financial support provided by the Research Niche Areas programme), the University of the Witwatersrand (Science Faculty Research Council) and the Mellon Foundation. The sponsors played no role in study design; in the collection, analysis and interpretation of data; in the writing of the report; and in the decision to submit the paper for publication. CL thanks for the Mellon Foundation for a postgraduate Mellon Fellowship. Mr R Mampa (University of the Witwatersrand) and Mr B Moolman and Dr M Stander (University of Stellenbosch) are thanked for providing the NMR and HRMS MS spectroscopy services, respectively.

References

[1] A. Jemal, R. Siegel, E. Ward, Y. Hao, J. Xu, M.J. Thun, Cancer statistics, 2009, CA Cancer J Clin 59 (2009) 225–249.
[2] J. Wils, Adjuvant treatment of colon cancer: past, present and future, J. Chemother. 19 (2007) 115–122.
[3] J.F. Kerr, A.H. Wyllie, A.R. Currie, Apoptosis: a basic biological phenomenon with wide-ranging implications in tissue kinetics, Br. J. Cancer 26 (1972) 239–257.
[4] G. Denecker, D. Vercammen, W. Declercq, P. Vandenabeele, Apoptotic and necrotic cell death induced by death domain receptors, Cell. Mol. Life Sci. 58 (2001) 356–370.
[5] G. Kroemer, J.C. Reed, Mitochondrial control of cell death, Nat. Med. 6 (2000) 513–519.
[6] G. van Loo, H. Demol, M. van Gurp, B. Hoorelbeke, P. Schotte, R. . Beyaert, B. Zhivotovsky, K. Gevaert, W. Declercq, J. Vandekerckhove, P. Vandenabeele, A matrix-assisted laser desorption ionization post-source decay (MALDI-PSD) analysis of proteins released from isolated liver mitochondria treated with recombinant truncated bid, Cell Death Differ. 9 (2002) 301–308.
[7] H. Chang, X. Yang, Proteases for cell suicide: functions and regulation of caspases, Microbiol. Mol. Biol. Rev. 64 (2000) 821–846.
[8] A.W. Abu-Qare, M.B. Abou-Donia, Biomarkers of apoptosis: release of cytochrome c, activation of caspase 3, induction of 8-hydroxy-2V-deoxyguanosine, increased 3-nitrotyrosine, and alteration of p53 gene, J. Toxicol. Environ. Health Part B. 4 (2001) 313–332.
[9] X. Saelens, N. . Festjens, L. Van de Walle, M. van Gurp, G. van Loo, P. Vandenabeele, Toxic proteins released from mitochondria in cell death, Oncogene 23 (2004) 2861–2874.
[10] M. Tolomeo, D. Simoni, Drug resistance and apoptosis in cancer treatment: development of new apoptosis-inducing agents active in drug resistant malignancies, Curr. Med. Chem. Anti-Cancer Agents 2 (2002) 387–406.
[11] (a) A. Doming, I. Ugi, Multicomponent reactions with isocyanides, Angew. Chem. Int. Ed. 39 (2000) 3168–3210;
(b) J. Zhu, H. Bienaymé (Eds.), Multicomponent Reactions, Wiley-VCH, Weinheim, 2005.
[12] For a short review see C. Enguehard-Gueiffier, A. Gueiffier, Recent progress in the pharmacology of imidazo[1,2-a]pyridines, Mini-Rev. Med. Chem. 7 (2007) 888–899.
[13] A.R. Katritzky, Y.-J. Xu, H. Tu, Regiospecific synthesis of 3-substituted imidazo [1,2-a]pyridines, imidazo[1,2-a]pyrimidines, and imidazo[1,2-c]pyrimidine, J. Org. Chem. 68 (2003) 4935–4937 and references therein.
[14] A.L. Rousseau, P. Matlaba, C.J. Parkinson, Multicomponent synthesis of imidazo[1,2-a]pyridines using catalytic zinc chloride, Tetrahedron Lett. 48 (2007) 4079–4082.
[15] K.S. Gudmundssen, B.A. Johns, Imidazo[1,2-a]pyridines with potent activity against herpesviruses, Bioorg. Med. Chem. Lett. 17 (2007) 2735–2739.
[16] L.R. Odell, M.T. Nilsson, J. Gising, O. Lagerlund, D. Muthas, A. Nordqvist, A. Karlén, M. Larhed, Funtionalized 3-amino-imidazo[1,2-a]pyridines: a novel class of drug-like *Mycobacterium tuberculosis* glutamine synthetase inhibitors, Bioorg. Med. Chem. Lett. 19 (2009) 4790–4793.
[17] R.B. Lacerda, C.K. de Lima, L.L. de Silva, N.C. Romeiron, A.L. Miranda, E.J. Barreiro, C.A. Frago, Discovery of novel analgesic and anti-inflammatory 3-arylamine-imidazo[1,2-a]pyridine symbiotic prototypes, Bioorg. Med. Chem. 17 (2009) 74–84.
[18] H. Kishino, M. Moriya, S. Sakuraba, T. Sakamoto, H. Takahashi, T. Suzuki, R. Moriya, M. Ito, H. Iwaasa, N. Takenaga, A. Ishihara, A. Kanatani, N. Sato, T. Fukami, Discovery of imidazo[1,2-a]pyridines as potent MCH1R antagonists, Bioorg. Med. Chem. Lett. 19 (2009) 4589–4593.
[19] S. Husinec, R. Markovic, M. Petkovic, V. Nasufovic, V. Savic, A base promoted cyclization of N-propargylaminopyridines. Synthesis of imidazo[1,2-a]pyridines derivatives, Org. Lett. 13 (2011) 2286–2289.
[20] For recent patents see for example: (a) A.M.M. Mjalli, A. Hari, B. Gaddam, D.R. Gohimukkula, D.R. Polisetti, H. El Abdellaoui, M. Rao, R.C. Andrews, R. Xie, T. Ren, Preparation of imidazo[1,2-a]pyridines as β-secretase inhibitors, PCT Int. Appl. (2010) WO 2010126745; A1 20101104;
(b) M. Dahlstroem, Preparation of imidazopyridine derivatives which inhibit the secretion of gastric acid, PCT Int. Appl. (2010) WO2010063876; A120100610;
(c) S. Allen, F.P. Marmsater, J.E. Robinson, S.T. Schlachter, J.P. Lyssikatos, Preparation of imidazo[1,2-a]pyridines as receptor tyrosine kinase inhibitors, PCT Int. Appl. (2010) WO2010039825; A220100408.
[21] I. Vermes, C. Haanen, C.P.M. Reutelingsperger, A novel assay for apoptosis: flow cytometric detection of phosphatidylserine expression on early apoptotic cells using fluorescence labelled annexin V, J. Immunol. Methods 180 (1995) 39–52.
[22] S. Fulda, Caspase 8 in cancer biology and therapy, Cancer Lett. 281 (2009) 128–133.
[23] N. Johnson, T.T.C. Ng, J.M. Parkin, Camptothecin causes cell cycle perturbations within T-lymphoblastoid cells followed by dose dependent induction of apoptosis, Leuk. Res. 21 (1997) 961–972.
[24] T. Mossman, Rapid colorimetric assay for cellular growth and survival: application to proliferation and cytotoxicity assays, J. Immunol. Methods 65 (1983) 55–63.